Title
X-Ray Magnetic Circular Dichroism Spectroscopy and Microscopy

Journal
Bulletin of the Materials Research Society, 20(10)

Authors
Smith, N.V.
Padmore, H.A.

Publication Date
1995-04-12

LBL-37135
UC-410
Preprint

Lawrence Berkeley Laboratory
UNIVERSITY OF CALIFORNIA

Accelerator & Fusion Research Division

Submitted to MRS Bulletin

X-Ray Magnetic Circular Dichroism Spectroscopy and Microscopy

N.V. Smith and H.A. Padmore

April 1995

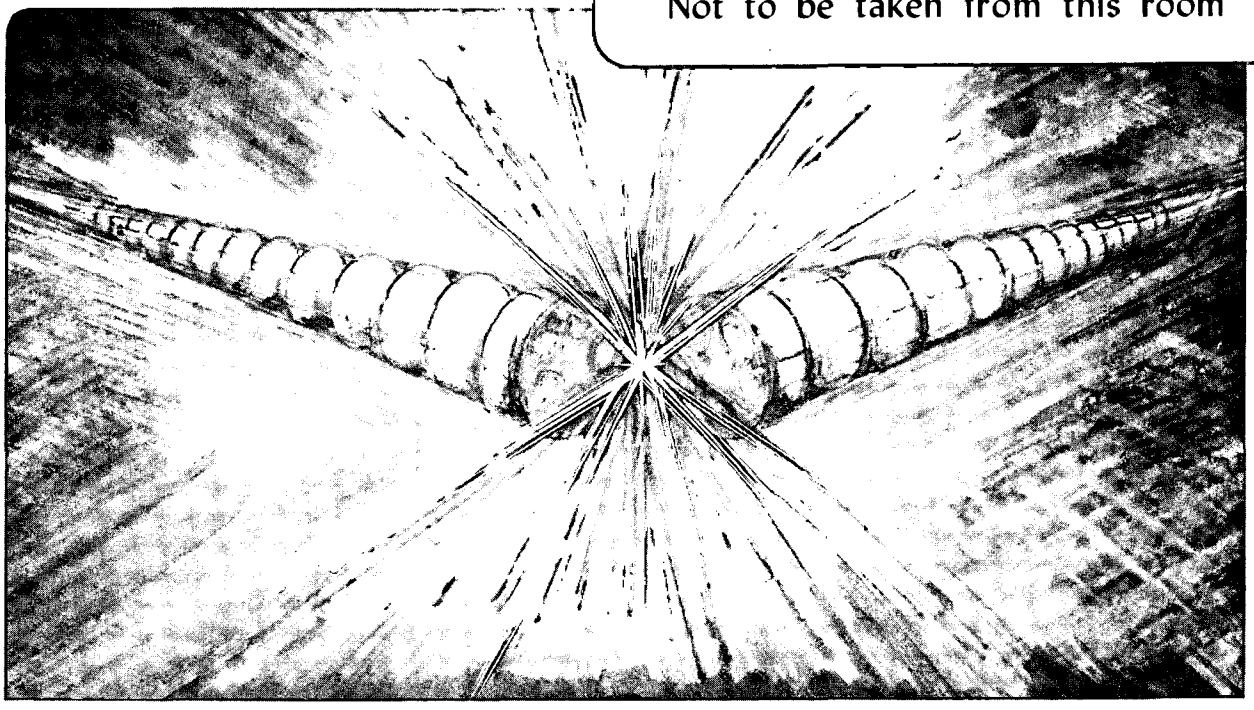

Prepared for the U.S. Department of Energy under Contract Number DE-AC03-76SF00098

DISCLAIMER

LBL-37135
UC-410

X-RAY MAGNETIC CIRCULAR DICHROISM SPECTROSCOPY AND MICROSCOPY*

N.V. Smith, H.A. Padmore

Advanced Light Source
Accelerator and Fusion Research Division
Lawrence Berkeley Laboratory
University of California
Berkeley, CA 94720, USA

Paper invited by the Bulletin of the Materials Research Society, April 1995

*This work was supported by the Director, Office of Energy Research, Office of Basic Energy Sciences, Materials Sciences Division, of the U.S. Department of Energy, under Contract No. DE-AC03-76SF00098.

X-ray Magnetic Circular Dichroism Spectroscopy and Microscopy

N. V. Smith and H. A. Padmore

Advanced Light Source, Lawrence Berkeley Laboratory, Berkeley, California 94720

Introduction

The advent of electron accelerators dedicated to the production of high intensity x-rays has revitalized experimental techniques based on x-ray absorption. A recent variant is to use *circularly polarized* x-rays generated either by use of out-of-plane radiation from a bending magnet or from a specially designed "insertion device". This new field of X-ray Magnetic Circular Dichroism (XMCD) shows considerable promise in spectroscopy and microscopy of magnetic materials. In this article we describe the nature of XMCD, offer a few examples of recent progress, and review the prospects for the future development using the newly constructed Advanced Light Source (ALS).

In the x-ray absorption process, a core electron is excited to a higher unoccupied level. By scanning the energy of the incoming x-ray photons through a core-level edge, we can probe the unoccupied density of states. For the 3d transition metals, the absorption edges of choice are the L_2 and L_3 edges corresponding respectively to transitions from the spin-orbit split $2p_{1/2}$ and $2p_{3/2}$ core levels to the 3d valence band. Such transitions are strongly dipole allowed, and the 3d valence states are central to magnetic behavior in these materials. The unoccupied 3d levels reside in a narrow enery range just above the Fermi level, so the near edge absorption spectrum consists of narrow lines as illustrated in the upper panel of Fig. 1 for the case of Ni.

XMCD is measured by recording the difference in the near edge spectrum for circularly polarized incident x-rays of left and right helicities. This is illustrated for Ni in the lower panel of Fig.1 which shows a negative spike at the L_3 edge and a positive spike at the L_2 edge. The information contained in the XMCD spectrum is element specific since different elements have different core level binding energies. It also directly gives the local vector magnetization of a sample, and in combination with sum rules described later, can give information on the orbital and spin contributions to the magnetic moment.

The $L_{2,3}$ absorption edges of the 3d transition metals lie in the soft x-ray energy region at photon energies from around 500 to 900 electron volts. The ALS is an ultrahigh brightness source which has been optimized for the photon energy range 100 to 1500eV which encompasses these $L_{2,3}$ edges and also the $M_{4,5}$ edges of the magnetically interesting rare earth elements. Circularly polarized soft x-rays from a high brightness synchrotron radiation source such as the ALS opens up the possibility of the use of XMCD *microscopy* to measure local magnetic properties of materials. We will address such prospects towards the end of this paper.

Synchrotron radiation.

Synchrotron radiation is produced by the acceleration of a relativistic electron as it is constrained to stay in a circular orbit by a magnetic dipole field. The spectrum thus created is a continuum extending from the far infra-red to the x-ray region. The distribution of light within this range depends on the electron energy and the magnetic dipole field, and for the ALS, with parameters of 1.5 GeV and 1.07 Tesla respectively, the peak of the distribution is around 500 eV. The relativistic nature of the electron beam also causes the light to be radiated within a small range of angles (the instantaneous opening angle), typically a fraction of a milliradian. When viewed in the plane of the electron orbit the light is plane polarized in the orbit plane, but when viewed out of the plane there is an appreciable circular component. Alternation between left and right helicity is achieved by switching between above and below plane.

Third generation of synchrotron radiation sources such as the ALS are specifically designed to optimize the brightness of the radiation. This is accomplished in two ways, firstly by reducing the angle and position space occupied by the electron beam (reduction of emittance), and by the use of undulator radiation sources. An undulator consists of an array of permanent magnets arranged to give an alternating vertical magnetic field with a period of a few centimeters. These devices are located in a straight section of the storage ring between dipole magnets. As the electron beam passes through such a device it oscillates in the horizontal plane and radiates. If the angular oscillation is smaller than the instantaneous opening angle, light emitted from one period of the device can interfere with light from following periods resulting in the compression of the angular distribution of the light. This combined with the small electron beam size and divergence results in ultra-high brightness and a source with a high degree of spatial coherence. This coherence is of vital importance in efficiently creating a diffraction limited focus for application to x-ray microscopy.

In order to measure an x-ray absorption spectrum, the x-ray source has to be monochromatized and in the soft x-ray region, this is performed using a reflection grating. This is used in conjunction with relay mirror optics so that a small spot of monochromatized photons of selectable energy and of variable bandpass is delivered to the sample. A typical monochromator will adequately span from 200 - 1500 eV photon energy, covering all the absorption edges of interest in magnetic materials.

Selection rules in XMCD and spectroscopy of magnetic films

The optical selection rules for transitions from p-like core levels to d-like valence levels in a ferromagnetic metal are illustrated in the energy diagram of Fig.2. The 2p core evels are split by spin-orbit interaction into $p_{3/2}$ and $p_{1/2}$ levels. The density of states for the spin "up" electrons (ie, those electrons whose magetic moment is aligned parallel with the applied magnetic field) is shifted down in energy relative to that for the spin "down" electrons. The inherent spin asymmetry of this system leads to a difference in absorption for photon helicity aligned parallel or antiparallel to the magnetization.

The nature of XMCD spectra in Ni were considered quite early by Erskine and Stern [2]. However, they made the simplifying assumption that the spin-orbit splitting in the valence band could be neglected, and this led inflexibly to predictions that the intensity ratios of the L_3 to L_2 lines in the absorption spectrum should be 2:1 (identical with the degeneracies of the $2p_{3/2}$ and $2p_{1/2}$ core levels), and -1:1 in the dichroism spectrum. The latter prediction implies that the sum over the dichroism spectrum should be zero. Actual results [3] for Ni are shown in Fig. 1 where it can be seen that the absorption ratio is 2.6:1 and the dichroism ratio is -1.6:1. Thus the results demonstrate that spin-orbit splitting within the d band must be taken into account at the outset. Basically, the holes at the top of the d band are enriched in $d_{5/2}$ character which will favor the L_3 over the L_2 line, a point first made by Mott in 1949 [4]. The spin-orbit interaction mixes the spin and orbital magnetic moments. Thus a nonzero sum over the dichroism spectrum implies a nonzero orbital magnetic moment. Indeed, Thole et al.[5] have shown that there is a powerful sum rule of which can be used quantitatively to extract the orbital moment from the integral over the dichroism spectrum.

An application of these ideas was used in the work of Samant *et al* [6] which demonstrates and quantifies an induced spin polarization on Cu atoms in the Cu spacer layers of Co/Cu multilayers. This study was motivated by the desire to understand the oscillatory exchange coupling in magnetic multilayers. Spectra taken at the Co $L_{2,3}$ edges showed the expected XMCD for ferromagnetic Co, but

spectra taken at the Cu $L_{2,3}$ edge reveal the very interesting result of a nonzero XMCD signal indicating an induced magnetic moment on the Cu atoms. The same sign of the XMCD signal indicates that the Cu moments are aligned ferromagnetically with the Co film. Application of the aforementioned sum rule yields values for the orbital and spin magnetic moments, which in turn are found to agree with theoretical calculations that find that the magnetic Cu atoms are those at the Co/Cu interface itself.

The elemental specificity of XMCD has been exploited by Chen *et al* [7] to perform magnetometry in magnetic heterostructures. Fig 3 shows hysteresis curves for a Fe/Cu/Co trilayer sample obtained by monitoring the intensity of the Fe and Co L_3 XMCD feature as a function of applied magnetic field. It is seen that the Fe and Co hysteresis curves are quite different. The Fe layer shows a square hysteresis loop with a coercive field of 38 Oe and a saturation field of ~100 Oe. The Co layer shows a less abrupt loop with a larger coercive field of 201 Oe and a saturation field of ~450 Oe. The Fe loop is representative of a single film. The fine structure in the Co loop demonstrates that the Co film has two distinct components. The onset of the fine structures corresponds exactly with the abrupt switching of the Fe layer. The most likely explanation is that the Cu spacer layer has pinholes resulting in some direct contact between the Fe and Co. A thoroughly interdiffused FeCo alloy, by contrast, gives identical Fe an Co hysteresis loops. Fig.3 also shows how the complicated hysteresis loop obtained using conventional methods can be unambiguously decomposed to reveal subtle features not otherwise apparent.

Imaging using synchrotron radiation

There are many types of x-ray microscopy that fit into the general classifications of scanning and full field techniques, but here we refer only to those that have direct relevance to the study of magnetic systems using soft x-rays.

The full field technique is the analog of the transmission electron microscope. The first stage (condensor) consists of an optical system whose function is to monochromatize the broad band x-ray source, followed by condensing mirrors to produce a small illuminated field of view at the sample, typically around 50 μm in diameter. In the second stage (projector), the photoelectrons created by this illumination are focused and magnified by a small electrostatic electron microscope and the image recorded on an image intensified CCD camera. The microscope itself consists of a 3 element electrostatic immersion lens objective, followed by a 3 element unipotential projector lens[8]. As well as imaging, the microscope works as a crude energy filter, and is essentially only sensitive to the low

energy portion of the secondary electron kinetic energy distribution. This range of energies combined with the chromatic aberration of the system results in a spatial resolution of typically 100 nm for an extraction energy of 10 KV. In order to acquire an image with magnetic contrast, the photon energy is tuned to the peak of the dichroism spectrum, and a difference image is obtained from images recorded with opposite helicity. The technique is inherently fast with expected frame rates of greater than 10 Hz for an optimized ALS bending magnet source. A second generation of electrostatic microscope is now under development that should improve the spatial resolution to around 10 nm. These work by either energy filtering the image [9], or compensating for the chromatic aberration of the lens system with an equal and opposite chromatic aberration produced by an electron mirror [10]. At the 10 nm resolution that should be attainable with this type of aberration corrected microscope, the additional two or three orders of magnitude of flux density from an undulator source will be required to provide adequate illumination.

A scanning x-ray microscope uses a Fresnel zone plate lens to produce a microfocus on the sample. The zone plate is simply a circular diffraction grating positioned normal to the beam. Rays that strike the zone plate at distances progressively further from the axis have to be diffracted through a greater angle to reach the focus and therefore the spacing of the grating structure decreases from the center outwards. The ultimate resolution of the device is approximately given by the spacing of the outer most zone. Before reaching the zone plate, the beam is monochromatized using a reflection grating, and focused in the horizontal and vertical directions to a pinhole. This pinhole defines the spatial coherence, and is the object point for the zone plate. The zone plate however only collects and focuses the fraction of the beam that is spatially coherent. Undulators when used in ultra-low emittance storage rings can radiate a significant fraction of their output as coherent light and are therefore the source of choice for zone plate microscopy. State of the art zone plate microscopes have reached a spatial resolution of around 35 nm [11]. This resolution is representative of the width of the outermost zone, and as the precision of electron beam writing the zone plate lithographic mask improves, it is expected that the resolution will approach 10 nm in the next few years. Having formed the microfocused beam on the sample, an image is created by scanning the sample across the beam and recording the sample response. This response could be, as in the full field microscope, the total yield of electrons, or it could be x-ray fluorescence, primary core level photoelectrons, ion yield, valence band photoemission etc. The advantage of the scanning microscope over the full field electron microscope is therefore both flexibility, and at present spatial resolution. Its disadvantage is the serial nature of the acquisition, and hence slow speed. Even so, the time required to record an image at high resolution at the ALS is only of the order of a few seconds.

Examples of XMCD imaging

The combination of XMCD and microscopy has been applied by Stohr *et al* [12] to examining the magnetic bit structure of a magnetic recording disk. The magnetic material was a CoPtCr alloy and imaging was performed at the Co $L_{2,3}$ edge at around 780 eV. The disk material was from a standard commercial product and was covered with a 130 Å thick layer of carbon and a 40 Å thick layer of a fluorocarbon polymer. The latter is used as a lubricant between the disc and the recording head. Images were obtained 5 eV lower in energy than the L_3 edge, at the L_3 edge and at the L_2 edge, and for both cases of the magnetization being parallel and anti-parallel to the polarization direction. The first case revealed no dichroism, but just topographic detail, but the image recorded at the L_3 edge showed strong dichroism in the region of the recorded bit pattern. Fig 4 shows such an image. The bit pattern was recorded with individual bits being 10 μm wide and a range of lengths, 10 μm, 2μm and 1μm . One particularly interesting feature of this work was that even though the magnetic layer was buried under a 170 Å thick layer of carbon and lubricant, it was possible to obtain strong electron yield from the magnetic layer. This is due to the fact that the technique images low energy secondary electrons, and these have a large mean free path. The resolution of 1 μm obtained in this experiment was primarily limited by signal strength, but it should be noted that at the ALS we will have over a factor of 100 increase in photon flux density at the sample, allowing us to get to the 0.1 μm resolution range using a dipole magnet source, and significantly higher again using a circularly polarized undulator.

The above example of Stohr *et al* was for a bit pattern written with alternating in-plane magnetization. The sample geometry in this case had the light incident on the sample at a grazing angle of 20°, and so as XMCD is sensitive to the direction of magnetization, the magnetic contrast was high. This geometry is also sensitive to perpendicular magnetization, as demonstrated by Tonner el al [13], but as the magnetization is smaller in the direction of the photon polarization, the magnetic contrast is less. However, well resolved bit patterns were recorded at μm spatial resolution from Fe-Tb-Co thin films. In this system the magnetic moment of the Fe and Tb atoms are anti-ferrimagnetically coupled, causing a reversal in contrast between the images recorded at Fe $L_{2,3}$ and Tb $M_{4,5}$.

It is worthwhile pointing out that XMCD microscopy is complementary to other types of surface magnetic imaging such as Scanning Electron Microscopy with Polarization Analysis (SEMPA) and Spin Polarized Low Energy Electron Microscopy (SPLEEM). These techniques are capable of excellent

spatial resolution, but suffer from non-elemental specificity, and a small electron spin depolarization length. In addition to providing elemental specificity, XMCD can also potentially give site specific information from core level photoemission or absorption edge shifts.

Future XMCD microscopy at the ALS

The ALS was designed to accommodate undulators as its primary radiation sources, and to have an ultra-low emittance electron beam to maximize brightness. Brightness translates directly into the photon flux in a diffraction limited focus, and so is the figure of merit for zone plate based microscopes.

We are presently constructing a special type of undulator in which the magnet blocks are arranged so that an oscillating field is produced in both the vertical and horizontal planes. The resulting trajectory can either be a pure helix or be an elliptical helix and results in the radiation of circular or elliptically polarized light. This device will be tunable over a large energy range including the 3d transition metal $L_{2,3}$ edges and the rare earth $M_{4,5}$ edges, and will be used in conjunction with both full field and zone plate based scanning microscopes. Completion of this new facility at the ALS will be by the end of 1996. It is expected that image acquisition rates will be limited only by the scanning speed of the zone plate (or sample) and that even for monolayer coverage surface systems, image acquisition times will be only a few seconds. For full field imaging of similar systems, acquisition times will be a fraction of a second, this time limited primarily by the time needed to reverse the helicity of the light.

In addition to this new undulator beamline, we are constructing a dipole magnet beamline that will be used for full field photoemission microscopy. The two beamlines will be complementary in nature, the undulator line being predominantly used for scanning magnetic microscopy at the ultimate resolution of a zone plate, and the dipole magnet beamline being used for more modest spatial resolution work, but where the parallel nature of the imaging microscope can be used to advantage, such as in time dependent studies. We therefore expect to be able to offer a very powerful yet broad-based XCMD facility for use by the magnetic materials community.

Acknowledgments

This work is supported by the Director, Office of Energy Research, Office of Basic Energy Sciences, Materials Sciences Division of the U.S. Department of Energy under contract No. DE-AC03-76SF00098.

References

1. J. Stohr and Y. Wu, in *New Directions in Research with Third-Generation Soft X-ray Synchrotron Radiation Sources*, edited by A. S. Schlachter and F. J. Wuilleumier, NATO ASI Series, (Series E: Applied Sciences) Vol 254, p.221.
2. J. L. Erskine and E. A. Stern, Phys. Rev. B **12** (1975) 5016
3. C. T. Chen, F. Sette, Y. Ma and S. Modesti, Phys. Rev. B **42** (1990) 7262
4. N. F. Mott, Proc. Phys. Soc. London, A 62, 416 (1949).
5. B. T. Thole, P. Carra, F. Sette and G. van der Laan, Phys. Rev. Lett. **68** (1992) 1943
6. M. G. Samant, J. Stohr, S. S. Parkin, G. A. Held, B. D. Hersmeier, F. Herman, M. van Schilfgaarde, L. -C. Duda, D. C. Mancini, N. Wassdahl, and R. Nakajima, Phys. Rev. Lett., **72(7)** (1994) 1112
7. C. T. Chen, Y. U. Idzerda, H. -J. Lin, G. Meigs, A. Chaiken, G. A. Prinz, and G. H. Ho, Phys. Rev. B., **48** (1993) 642
8. B. P. Tonner, G. R. Harp, S. F. Koranda and J. Zhang, Rev. Sci. Instrum., **63** (1992) 564
   B. P. Tonner and D. Dunham, Nucl. Instrum. Meth. **A 347** (1994) 436
9. B. P. Tonner, Nucl. Instrum. Meth. A **291** (1990) 60
10. G. F. Rempfer, J. Appl. Phys. **67** (1990)6027
11. H. Ade, X. Zhang, S. Cameron, C. Costello, J. Kirz and S. Williams, Science **258** (1992) 972
    H. Ade, X. Zhang, C. Jacobsen, J. Kirz, S. Lindaas, S. Williams, and S. Wirick, Nucl. Instrum. Meth. **A 347** (1994) 431
12. J. Stohr, Y. Wu, B. D. Hermsmeier, M. G. Samant, G. R. Harp, S. Koranda, D. Dunham and B. P. Tonner, Science **259** (1003) 658
13. B. P. Tonner, D. Dunham, J. Zhang, W. L. O'Brien, M. Samant, D. Weller, B. D. Hermsmeier and J. Stohr, Nucl. Instrum. Meth. **347** (1994) 142

Captions

Fig 1 X-ray absorption and CMXD at the $L_{2,3}$ core-level edges of Ni taken with helicity directions of the photons and that of the majority 3d valence electrons parallel and antiparallel to each other.

Fig.2 Schematic energy level diagram for x-ray optical transitions from spin-orbit-split p core levels to magnetic-exchange-split d bands in a ferromagnetic metal.

Fig 3 Element specific magnetometry using MCD. The top panel shows the Fe and Co L_3 white line intensities as a function of the applied magnetic field for a Fe/Cu/Co trilayer sample. Note the fine features in the Co hysteresis curve. The bottom panel shows the comparison between an overall hysteresis curve obtained using conventional methods (solid line) and a linear combination fit of the element specific MCD hysteresis curves (dotted line); also shown are the constiuent Fe and Co contributions.

Fig. 4 Magnetic microscopy using MCD. The image is of magnetic domains on a CoPtCr magnetic recording disc produced by subtracting images taken at the L_3 and L_2 edges of Co using circularly polarized x-rays. The bit pattern rows are 10 μm tall, and decrease in width from 10 μ in the upper row through 2 μm to 1μm in the lower row. The magnetization direction of the domains lies along the rows.

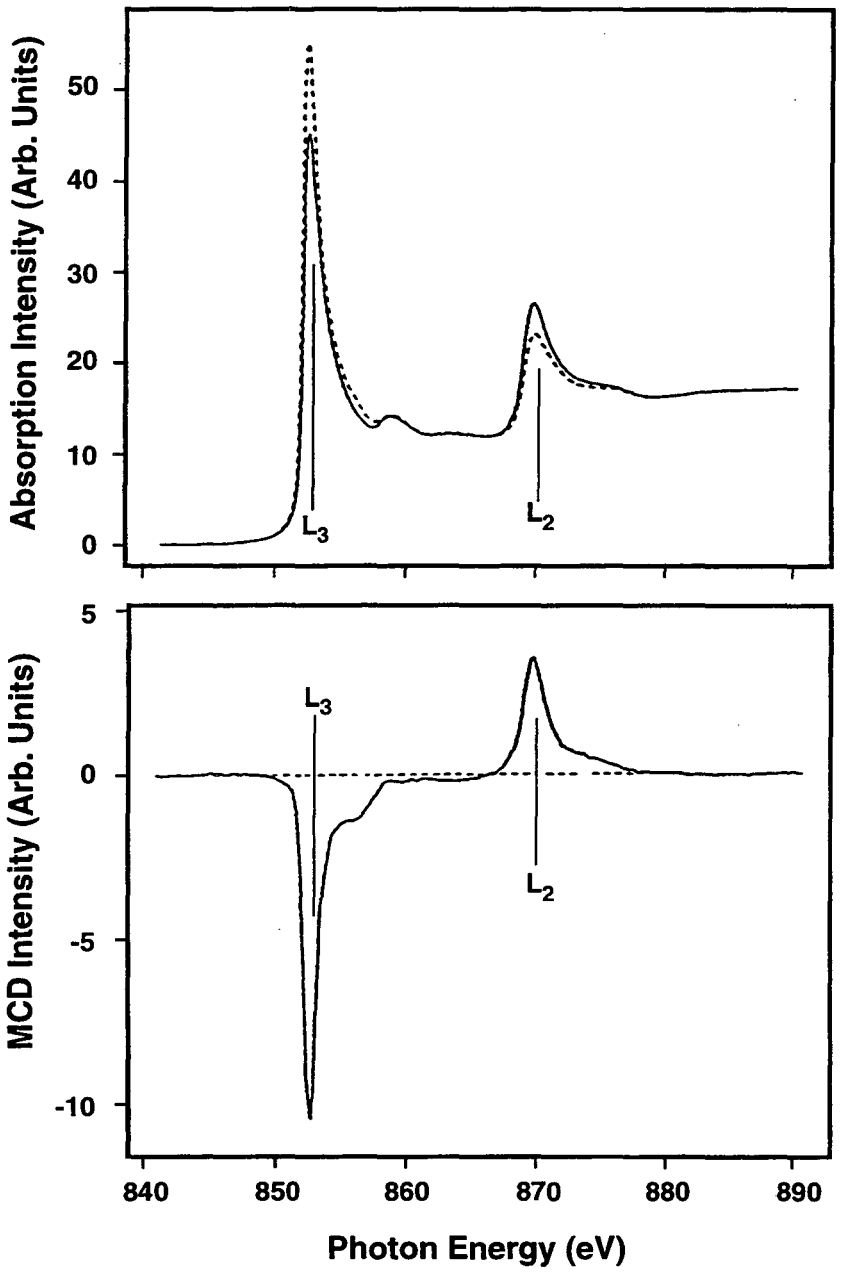
Absorption Intensity (Arb. Units)
50
40
30
20
10
0
L3
L2
MCD Intensity (Arb. Units)
5
0
-5
-10
L3
L2
840
850
860
870
880
890
Photon Energy (eV)

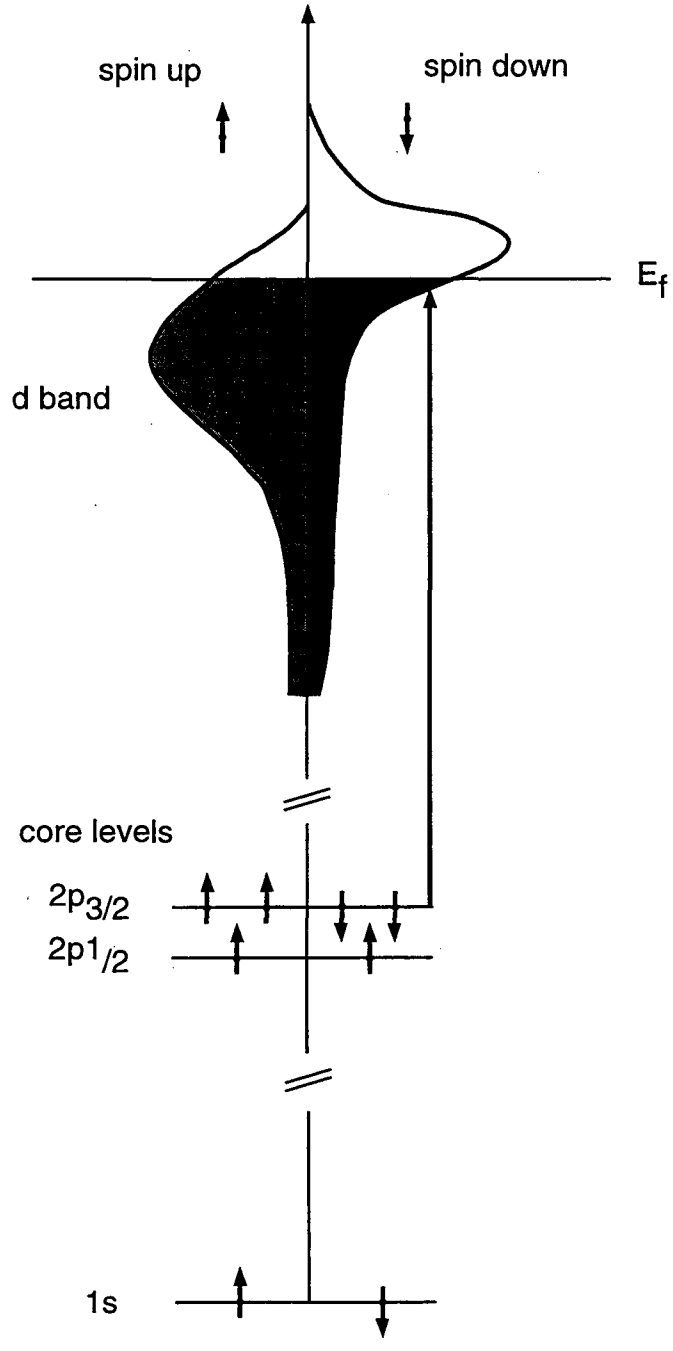
spin up
spin down
E_f
d band
core levels
$2p_{3/2}$
$2p1_{/2}$
1s

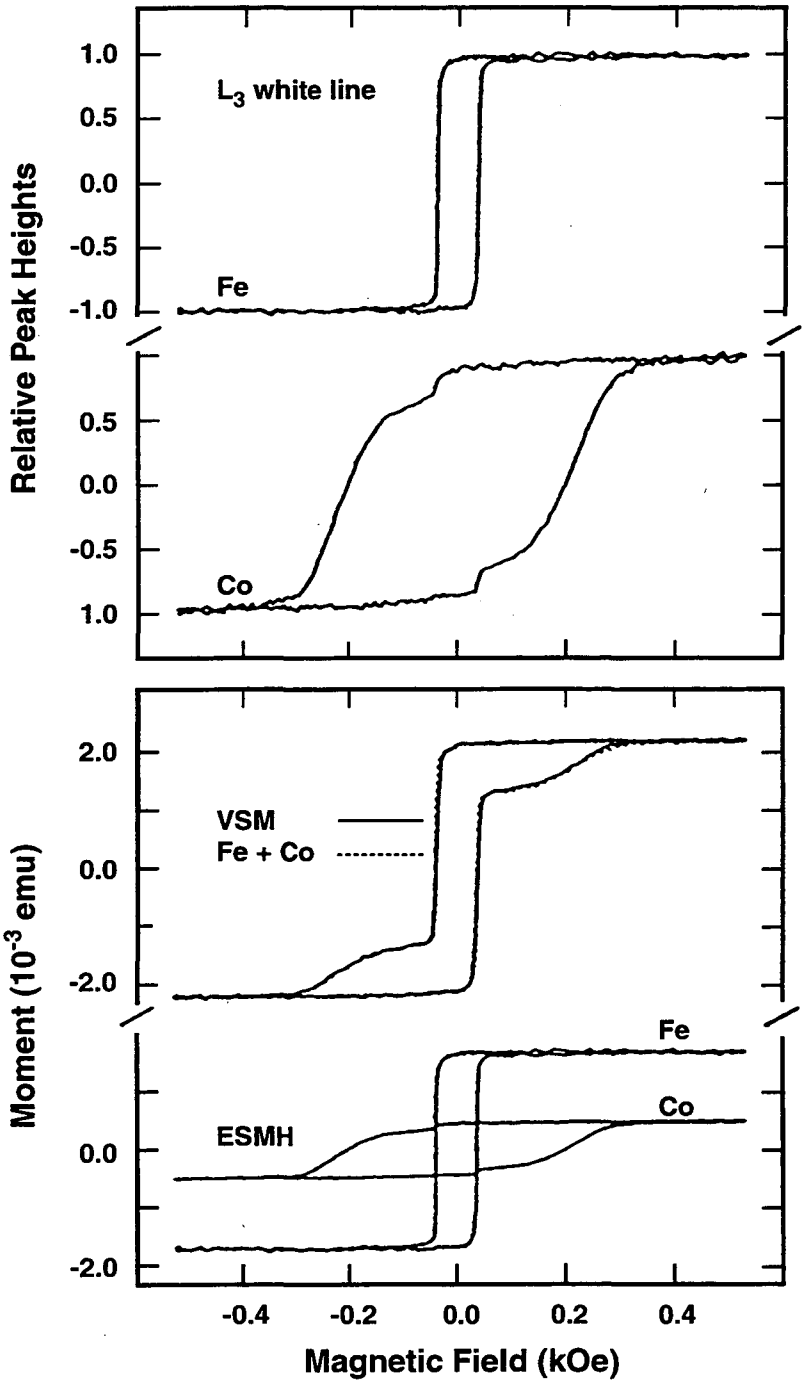
Relative Peak Heights
1.0
0.5
0.0
-0.5
-1.0
L_3 white line
Fe
0.5
0.0
-0.5
1.0
Co
Moment (10^{-3} emu)
2.0
0.0
-2.0
VSM
Fe + Co
Fe
Co
ESMH
0.0
-2.0
-0.4
-0.2
0.0
0.2
0.4
Magnetic Field (kOe)

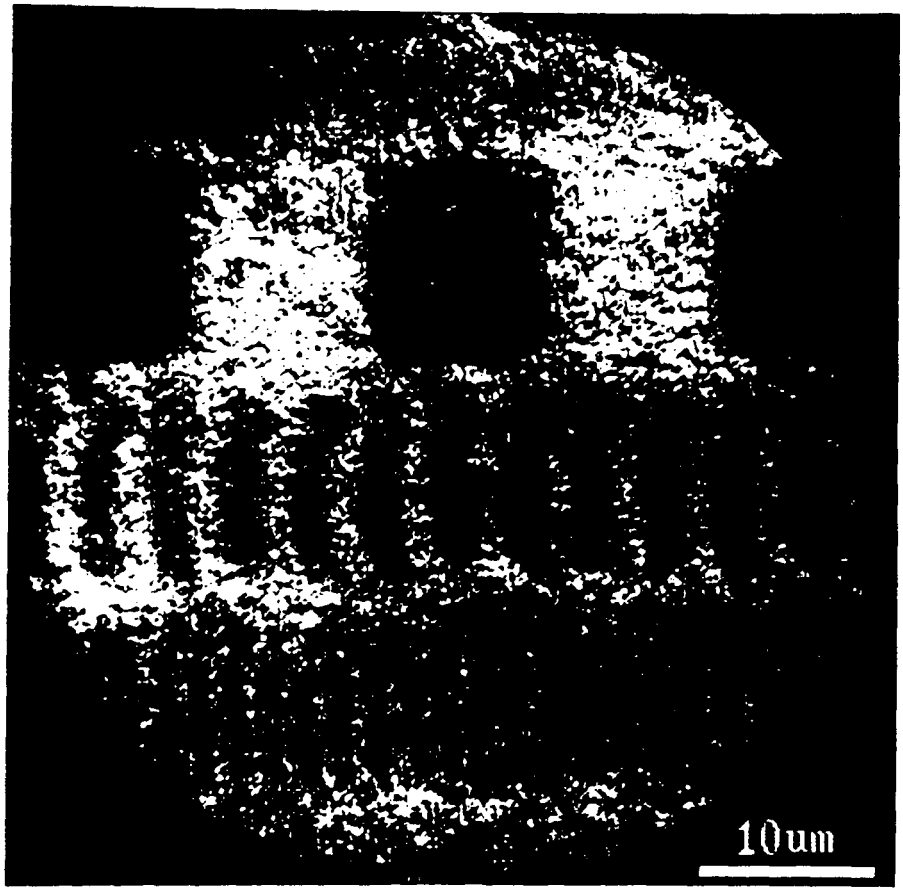
10um

LAWRENCE BERKELEY LABORATORY
UNIVERSITY OF CALIFORNIA
TECHNICAL AND ELECTRONIC
INFORMATION DEPARTMENT
BERKELEY, CALIFORNIA 94720